Microelectronic Engineering 86 (2009) 1876–1882

Contents lists available at ScienceDirect

Microelectronic Engineering

journal homepage: www.elsevier.com/locate/mee

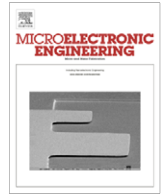

Understanding negative bias temperature instability in the context of hole trapping

T. Grasser [a,*], B. Kaczer [c], W. Goes [a], Th. Aichinger [d], Ph. Hehenberger [b], M. Nelhiebel [e]

[a] Christian Doppler Laboratory for TCAD in Microelectronics, Institute for Microelectronics, TU Wien, Gußhausstraße 27–29, A-1040 Wien, Austria
[b] Institute for Microelectronics, TU Wien, Gußhausstraße 27–29, A-1040 Wien, Austria
[c] IMEC, Leuven, Belgium
[d] KAI,Villach, Austria
[e] Infineon Technologies, Villach, Austria

ARTICLE INFO

Article history:
Received 3 March 2009
Received in revised form 15 March 2009
Accepted 15 March 2009
Available online 26 March 2009

Keywords:
Negative bias temperature instability
Reliability
Modeling hole trapping
Oxide charges
Interface states

ABSTRACT

Hole trapping is often considered a parasitic component clouding the real degradation mechanism that is responsible for the negative bias temperature instability (NBTI). As such, it is often dealt with in a rather sketchy way that lacks physical rigor. We review hole trapping mechanisms that go beyond the conventional elastic tunneling mechanism by including structural relaxation and field effects. Contrary to some previous studies, it is shown that the rich spectrum of experimentally observed features of the most commonly observed defect in amorphous oxides, the E' center, is consistent with experimental data available for NBTI. In particular, we show that a full model that includes the creation of E' centers from their neutral oxygen vacancy precursors and their ability to be repeatedly charged and discharged prior to total annealing is consistent with a first stage of degradation. In a second stage, positively charged E' centers can trigger the depassivation of P_b centers at the Si/ SiO_2 interface or K_N centers in oxynitrides to create an unpassivated silicon dangling bond. We formulate a complete model and evaluate it against experimental data.

© 2009 Elsevier B.V. All rights reserved.

1. Introduction

The current understanding of the negative bias temperature instability (NBTI) sees the creation of interface states and oxide charges as the main reason for device degradation following bias temperature stress [1–3]. However, nearly every aspect is controversial, ranging from the creation mechanism of interface states and their recovery behavior to the importance and mechanisms behind hole trapping. Existing models fail in explaining the temperature and voltage dependence of the recovery behavior and the experimentally observed correlation between interface and oxide charges [3], to name just a few. In particular, the popular reaction-diffusion theory [4], which assumes predominant creation of interface states controlled by the diffusion of molecular hydrogen in the oxide/polysilicon layers also fails for instance in reproducing fast recovery, recovery lasting considerably longer than the preceding stress, the bias and temperature dependence of the recovery, and the strong sensitivity to the stress duty-factor [3].

Before suggesting a new model, we briefly summarize some key experimental observations obtained by extended measure/stress/measure (eMSM) experiments [2], which provide important insights regarding the dynamics of NBTI. In particular, they can be used to effectively rule out a number of alternative models.

* Corresponding author.
E-mail address: Grasser@iue.tuwien.ac.at (T. Grasser).

0167-9317/$ - see front matter © 2009 Elsevier B.V. All rights reserved.
doi:10.1016/j.mee.2009.03.120

1.1. Scalability

The data recorded using the eMSM scheme can often be made to overlap by multiplication with a suitably chosen scaling factor. While the initial behavior up to about 1 s is well approximated by a logarithmic time dependence and the long-term data approximately follows a power-law, *the same scaling factor can be used in both regimes* [5]. A similar scalability is observed during recovery [5], which, to first-order, follows a logarithmic time dependence.

1.2. Bias and temperature dependence of stress

Degradation of devices subjected to short stresses of about 1 s follows $B_s(F,T)\log_{10}(t_s/t_0)$, whereas recovery can be fit by $B_r(F,T)\log_{10}(1+t_s/t_r)+P(t_s)$, P is a roughly permanent contribution. For what is typically considered NBTI stress in this oxide thickness range ($V_{stress} \leqslant -1$ V), the pre-factor B_s can be approximated as $B_s(F,T) \approx B_{s,0}T^{\Theta}F^2$, with $\Theta \approx 2$, see Fig. 1.

1.3. Asymmetry between stress and relaxation

It has been long understood that recovery takes substantially longer than the time used to build up the degradation. Using the extracted pre-factors B_s (fit to a log in the range 1 ms,...,1 s) and B_r (fit to a log in the range 1 ms, ...,100 ms) we observe that the ratio B_s/B_r is about 2.5, independent of temperature and voltage.

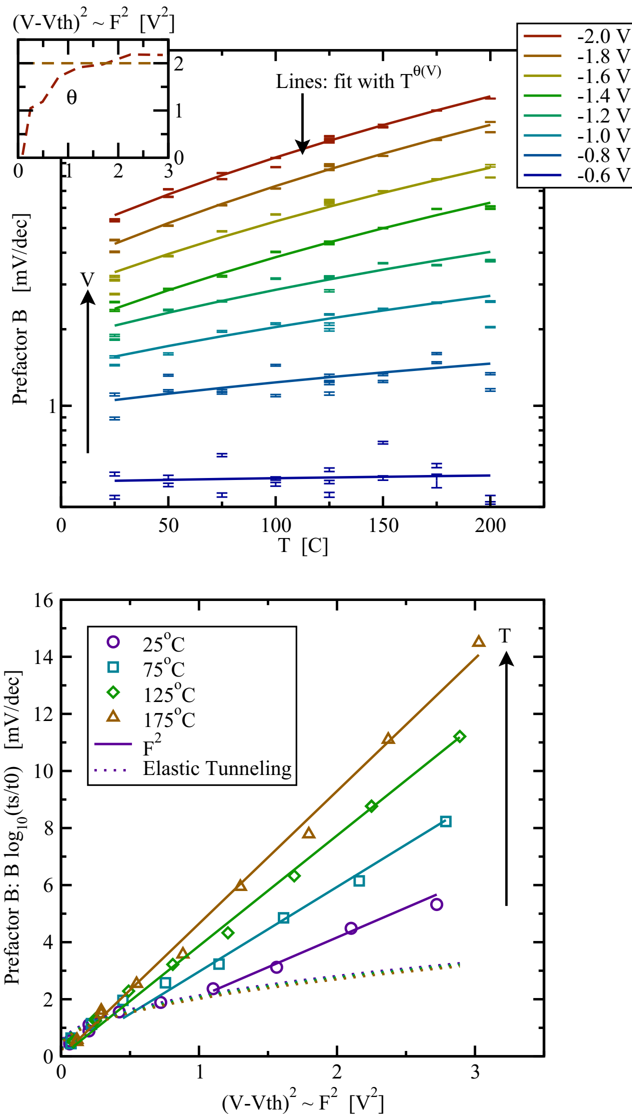

Fig. 1. PMOSFETs with EOT = 1.4 nm are subjected to various stress voltages and temperatures for 1 s. The degradation follows $B\log_{10}(t_s/t_0)$, with t_0 = 1 ms being the first OTF measurement point. Contrary to the predication of elastic tunneling theory, the prefactor B strongly depends on temperature (T^2) once a critical oxide field is reached (**top**, error bars are data, lines are fits). Also, the field dependence can be well approximated by F^2, with $F \sim V - V_{th}$ (**bottom**).

Although this asymmetry may look quite innocent at a first glance, it turns out to be a considerable challenge for any modeling attempt.

1.4. Bias dependence of recovery

Recovery has been shown to depend on the bias voltage applied during recovery [6,7,1,8]. In particular, application of positive bias accelerates recovery. Just as the asymmetry, this is also challenging to reproduce correctly by a quantitative model.

2. Hole trapping process

Hole trapping is often modeled using elastic tunneling into pre-existing traps located at various distances away from the interface. Elastic hole trapping is to first-order temperature independent and linearly dependent on the stress field [9]. Furthermore, the model predicts symmetric degradation and recovery behavior. As such, this is incompatible with our data and a different explanation has to be sought.

Of particular interest are hole trapping models that have been applied since the 1970s in attempts to understand 1/*f*-noise and thermally stimulated currents at semiconductor surfaces [10,11]. These models are based on a dispersion of activation energies which for a homogeneous distribution results in a 1/*f* behavior. In these models it is assumed that holes can be captured via a (*thermally activated*) multiphonon emission (MPE) process into deep near-interfacial states/border traps [12,13,9,11], probably into oxygen vacancies (E' centers) [11]. The MPE process differs from the conventionally invoked elastic tunneling process, notably due to its temperature activation and the larger time constants resulting therefrom [12].

In order to accomodate the field dependence, we have to recall that the MPE mechanism is derived under the assumption of negligible electric fields. This assumption is definitely violated in the case of NBTI. An extension of MPE to the large electric field case has been developed for the emission of particles from deep traps and known as *multiphonon-field-assisted tunneling (MPFAT)* [14,15]. The signatures of this mechanism are its $\exp(F^2/F_c^2)$ field dependence (note that only the logarithm of the enhancement factor enters B_s) and a considerable temperature activation (from the MPE process). The MPFAT process is schematically illustrated in Fig. 2: a hole can either be in the valence band or in a trapped state. These two states are represented by the two solid parabola which give the total energy of the system. The vibrational modes can be approximated using a simple oscillator model and at the intersection point a transition can occur. The intersection point determining the barrier ΔE_B is dramatically lowered by the application of an electric field, resulting in an enhancement of $\exp(F^2/F_c^2)$.

3. Properties of the E' center

In order to develop an accurate microscopic model for hole trapping in the context of NBTI, we summarize the most important features collected in a long line of studies on oxide defects which provides a solid basis for our NBTI model.

- The most likely microscopic candidate for the 'trapped hole' are defects from the E' center family, most notably the E'_γ center [16,17]. An E'_γ center is thought to be created when a hole is trapped in the precursor structure, which is commonly assumed to be a neutral oxygen vacancy.
- The energy level for hole trapping is roughly located at about 1 eV below the Si valence band [16], see Fig. 3.
- Once the silicon bond is broken, the distance between the two silicon atoms increases into a new equilibrium position, which requires a large-range structural relaxation of the surrounding lattice (10 Å [18]), and an E'_γ center is obtained. The E'_γ is visible in ESR (electron spin resonance) when positively charged, that is, right after hole capture.
- An important peculiarity of the E'_γ center is that it can be repeatedly charged and discharged. The corresponding energy-levels lie within the silicon bandgap [16]. The idea behind this cyclability is that once the hole is emitted (that is, an electron is captured), the bond between the two silicon atoms does not fully reform but the defect remains in a dipole state which can easily lose an electron again. The fact that the E' center can act as a switching trap was suggested by Lelis et al. [19] and led to the formulation of the Harry-Diamond-Laboratories (HDL) model of the E' center. The model was later confirmed by ESR studies [20] and theoretical calculations [21], see Fig. 4 for a schematic representation.

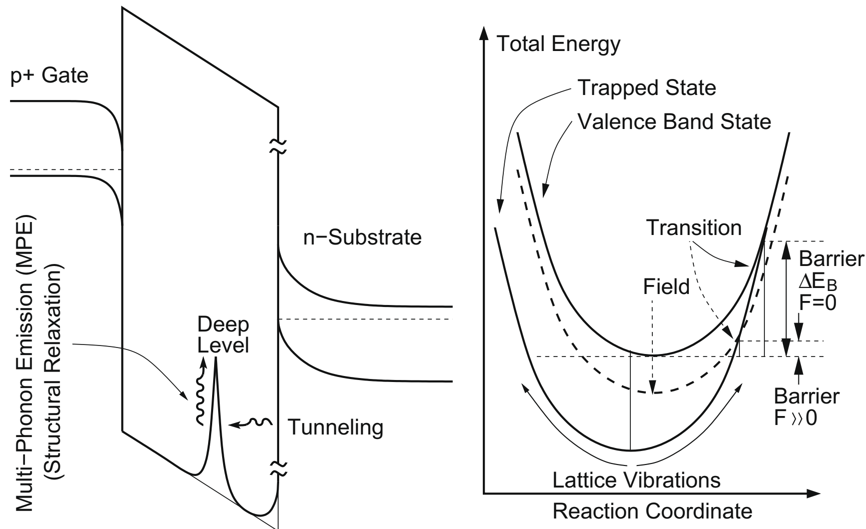

Fig. 2. The multiphonon-field-assisted tunneling (MPFAT) process used to explain the experimental data: elastic tunneling into deep states is only allowed when the excess energy of holes can be released via a multiphonon emission process during structural relaxation. The probability for a thermionic transition over the barrier ΔE_B has been estimated as $\exp(-\beta\Delta E_B)$ using 1D reaction-coordinate calculations [12,15], with $\beta = 1/k_BT$. Application of an electric field shifts the total energy of the valence band state (dashed line), increasing the transition probability by $\exp(F^2/F_c^2)$ [14,15].

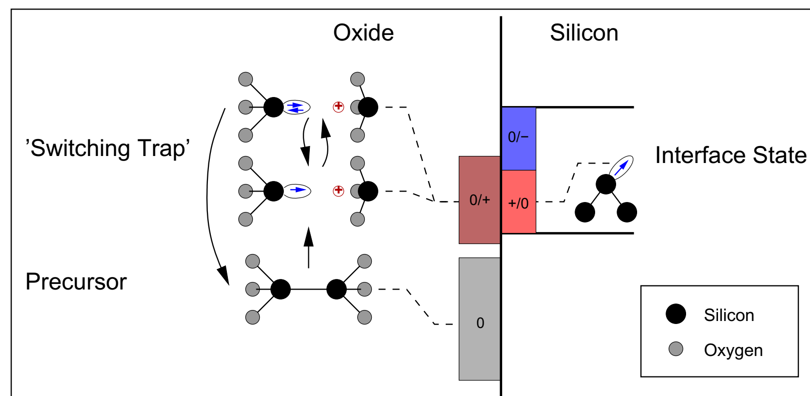

Fig. 3. Electronic energy-levels required in the Harry-Diamond-Laboratories (HDL) model and in our two stage model: the neutral precursors lie about 1 eV below the silicon valence band edge. The E'_γ levels are assumed to be inside the silicon bandgap, while for simplicity both the charged and the uncharged level are assumed to be roughly identical. Interface states are assumed to introduce amphotheric defects into the silicon band-gap. All electronic energy-levels are assumed to be homogeneously distributed due to the amorphous nature of the interfacial layer.

- Only after having been in its electrically neutral state for a while, the structure relaxes again to the initial dimer configuration and the defect is completely healed.
- The E'_γ is often considered a donor-like defect [16], that is, it is either neutral (ESR inactive) or positively charged (ESR active).
- The oxygen vacancy can also act as an electron trap, with a trap level close to the silicon conduction band [21,22].
- Due to the amorphous nature of the interfacial layer, a considerable distribution of the energy-levels is to be expected.

The above summary bears some important and interesting consequences regarding our understanding of NBTI:

- So far, hole trapping has been mainly considered as being into pre-existing traps which rapidly fill but are not related to the actual NBTI mechanism, a somewhat parasitic component which has to be removed to get to the heart of NBTI [23].
- Using CV measurements, NBTI has been shown to be due to donor-like defects [24,25,23]. In contrast to interface states, which are amphotheric, that is, donor-like only in the lower half of the silicon band-gap, the E'_γ center is considered a donor-like defect [16].
- NBTI recovery is strongly bias-dependent, in particular when the gate voltage is moved from inversion into accumulation [6]. This is intuitively consistent with carrier trapping [26].
- Describing hole trapping via the known properties of the E' center *promotes the positive oxide charge component* from a purely parasitic component to the *central contributor* to NBTI. Indeed, some key experimental features of NBTI which are incompatible with the P_b center and simple hole trapping models follow directly from the properties of the E' center.
- The amount of positive charge visible and thus contributing to ΔV_{th} will depend on the position of the Fermi-level, that is, the gate voltage at which the degradation is monitored. For example, during OTF experiments, the Fermi-level is below the valence band edge and most defects will be positively charged (state 2 in Fig. 4) and thus visible. During recovery, the Fermi-level is moved towards mid-gap and a smaller frac-

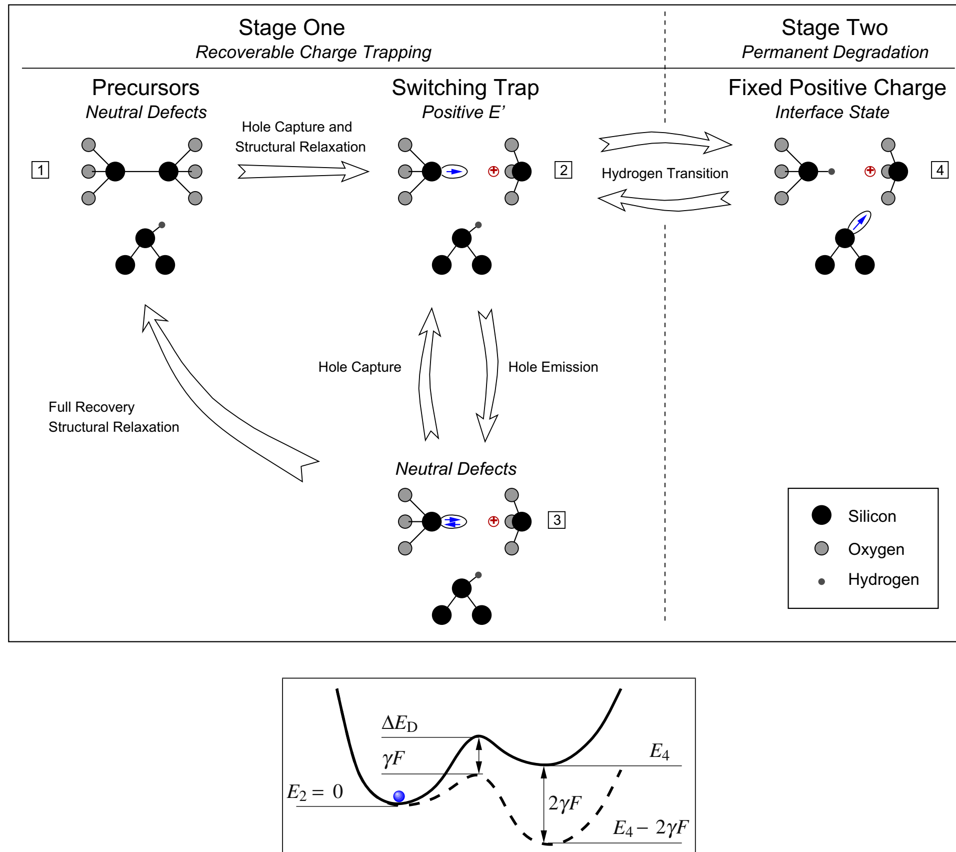

Fig. 4. Left: The HDL model for a switching oxide trap coupled to the creation of a dangling bond at the interface. When the E' center is positively charged (in state 2), the hydrogen passivating a silicon dangling bond at the interface can move to the E' center, thereby effectively locking in the E' center (state 4). The charge state of the thereby created dangling bond depends on the position of the Fermi-level. **Bottom**: The transition between states 2 and 4 is modeled by assuming a field-dependent thermal transition over a barrier.

tion of the defects will be positive and visible. This occupancy effect will manifest itself as a change in the subthreshold slope, and is consistent with recent experimental results [27,26].

- Since full annealing of oxide defects is only possible when the defect is neutral (state 3), defects having an electrically higher trapping level will show a slower recovery rate. Indeed, this is fully compatible with what is observed during NBTI recovery and explains the often observed bias dependence. Furthermore, this can explain the asymmetry between stress and recovery, with the recovery lasting considerably longer than the time required to build up the degradation.
- The fact that the precursor level is below the valence band and the defect level within the silicon bandgap is precisely what is expected of a defect responsible for NBTI. A higher energy level of the precursor, e.g. above the valence band, would cause most precursors to be already initially broken in PMOSFETs. The energy level of the created defect inside the silicon bandgap results in most defects to be positively charged (a donor-like defect) during both stress and recovery. A lower defect level would render the defects electrically neutral and thus not contributing to the threshold voltage shift.
- After NBTI stress an increase in $1/f$ noise has been reported [28,29]. The prime suspect for $1/f$ noise are the E' centers [21,11], while P_b centers do not create a suitable $1/f$ spectrum.

Although an extensive amount of literature is available on the E' center and its qualitative behavior is well understood, no rate-equation based model that spans the full cycle of trap creation, recharging and discharging until final annealing seems to be available. However, for NBTI a full model is required in order to account for the asymmetry between stress and relaxation and the correct bias dependence of recovery [30].

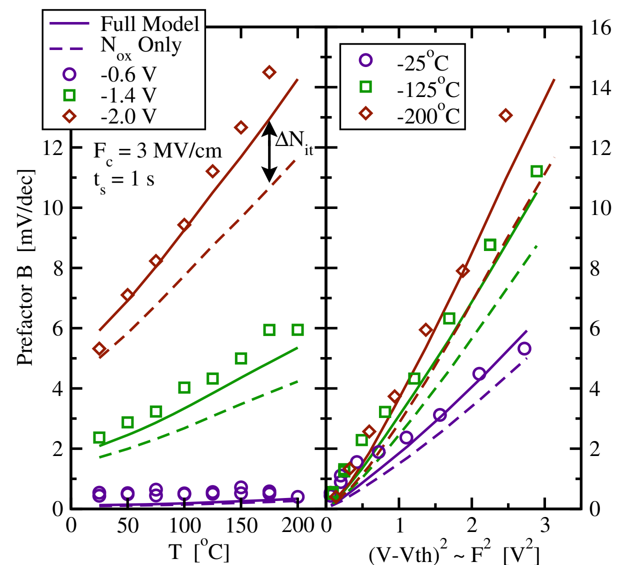

Fig. 5. The measured prefactor $B_s(F,T)$ of Fig. 1 compared to the simulated prefactor of the two stage model obtained under the same conditions. Very good agreement for all voltages and temperatures is obtained. Since the two stage model captures the asymmetry, good agreement during both stress and recovery is possible. We put the remaining deviation down to the mobility error in the OTF data [34].

4. A two stage model

Based on the above observations we formulate a *new model for NBTI*, where defect creation proceeds via a *two stage process*: In stage one, upon application of stress, holes can be trapped into near-interfacial oxygen vacancies via the MPE/MPFAT mechanism. In the second stage, the increased hole concentration considerably enhances the creation of poorly recoverable defects, e.g. P_b-centers in SiO_2 layers and K_N-centers in oxynitrides [31].

Our full model for the E' switching trap relies heavily on the HDL switching trap model [19]. In order to capture this coupling between E' and P_b centers we extend the HDL model by introducing an E'/P_bH complex. The complex is assumed to be in one of 4 states, with states 1–3 describing the dynamics of the E' center and the P_b center being passivated with H (see Fig. 4). Once positively charged (state 2), the E' center can attract the H from the P_bH. When this happens, the E'/P_b H complex moves to state 4. This step locks in the E' center and creates a dangling bond at the interface, whose charge state quickly follows the Fermi-level in the substrate. The H has a non-zero probability of moving back to the P_b center, thereby resetting the E'/P_b complex to state 2, from which complete annealing is eventually possible.

Alternatively, it might be possible that the hole capture event into the E' center releases atomic hydrogen which then depassivates a passivated interface state by forming H_2 [32]. As the microscopic details of the coupling mechanism are not evident from the data available to us at the moment, we anticipate some refinement of our model. However, we expect the resulting equation systems to be of a similar form as the one suggested below.

The rate-equation describing such a E'/P_bH complex follow in a straight-forward manner from Fig. 4

$$\frac{\partial f_1}{\partial t} = -f_1 k_{12} + f_3 k_{31}, \tag{1}$$

$$\frac{\partial f_2}{\partial t} = +f_1 k_{12} - f_2 k_{23} + f_3 k_{32} - f_2 k_{24} + f_4 k_{42}, \tag{2}$$

$$\frac{\partial f_3}{\partial t} = +f_2 k_{23} - f_3 k_{32} - f_3 k_{31}, \tag{3}$$

$$\frac{\partial f_4}{\partial t} = +f_2 k_{24} - f_4 k_{42}. \tag{4}$$

Naturally, (1)–(4) are not linearly independent since the defect has to be in one of its four states ($f_1 + f_2 + f_3 + f_4 = 1$). The probability of being in state i is given by f_i while the transition rates from state i to j are given by k_{ij}. The rates k_{ij} are formulated using a generalization

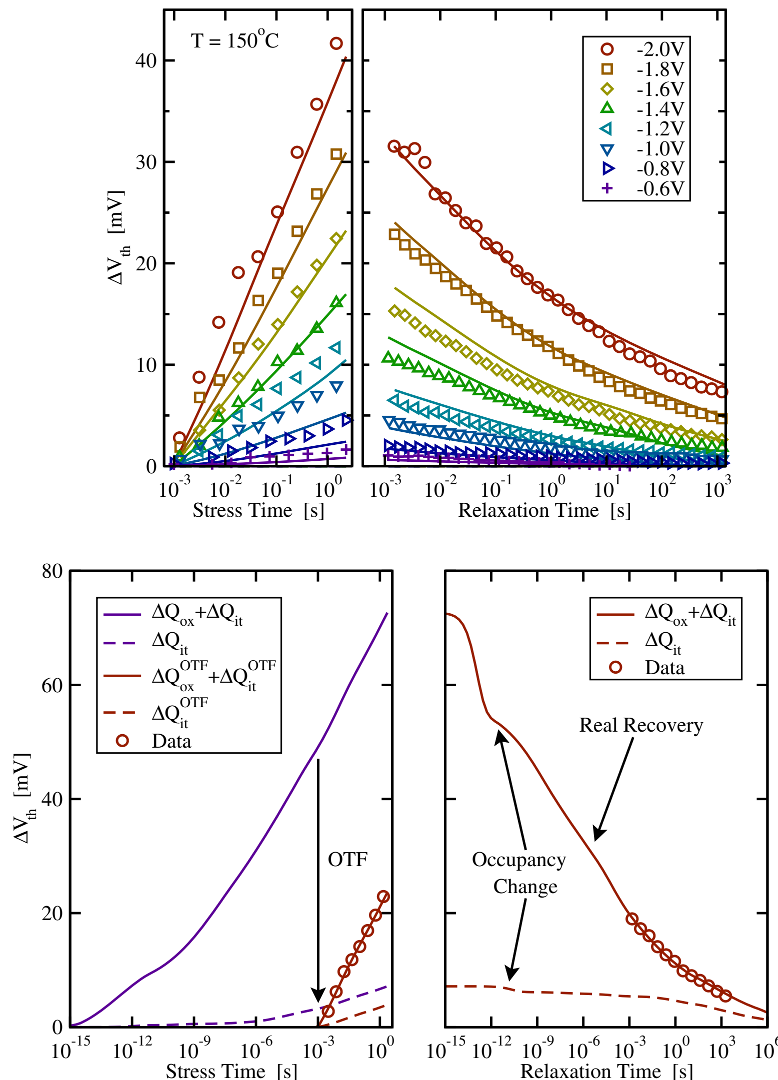

Fig. 6. Top: Comparison of the simulated asymmetry of stress and recovery measured at 150 °C for 8 different stress voltages for the thin SiON devices. The asymmetry is properly reproduced by the model, resulting in a good fit during *both* stress and recovery. **Bottom**: Detailed simulation results at 50 °C and −2 V. Both measurements are taken at 1 ms and miss about 50 mV of the real degradation.

of the lattice-relaxation multiphonon emission (MPE) theory for phonon-assisted capture of holes and electrons [12,9] by including a depth dependence and MPFAT field acceleration [14,15].

Consider a trap level E_T located at a distance x away from the interface. The hole capture and emission rates are then approximately given by

$$k_p^c = p v_p^{th} \sigma_p e^{-x/x_{p,0}} e^{-\beta\Delta E} \theta(E_{VT}, e^{-\beta E_{VT}}, 1) e^{F^2/F_c^2}, \tag{5}$$
$$k_p^e = p v_p^{th} \sigma_p e^{-x/x_{p,0}} e^{-\beta\Delta E} \theta(E_{VT}, e^{-\beta E_{VF}}, e^{-\beta E_{TF}}), \tag{6}$$

while the corresponding rates for electrons read

$$k_n^c = n v_n^{th} \sigma_n e^{-x/x_{n,0}} e^{-\beta\Delta E} \theta(E_{TC}, e^{-\beta E_{TC}}, 1), \tag{7}$$
$$k_n^e = n v_n^{th} \sigma_n e^{-x/x_{n,0}} e^{-\beta\Delta E} \theta(E_{TC}, e^{-\beta E_{FC}}, e^{\beta E_{TF}}). \tag{8}$$

Here, p and n are the hole and electron concentrations in the channel, v_p^{th} and v_n^{th} their thermal velocities ($\sqrt{8k_BT/(\pi m)}$), σ_p and σ_n their capture cross sections ($\sim 3\times 10^{14}\,\mathrm{cm}^2$ [33]), E_F the Fermi-level in the channel, E_V and E_C the valence and conduction bands directly at the interface (classical approximation), ΔE the MPE barrier, and $\beta = 1/k_BT$. F_c is the reference field for the multiphonon-field-assisted tunneling mechanism which is, due to lack of decisive data, only introduced for hole capture. According to a simplified WKB approximation for large tunneling barriers ϕ [9], $x_0 = \hbar/(2\sqrt{2m\phi})$, $x_{n,0} = 0.8$Å for electrons ($\phi_C \approx 3.2$eV and $m \approx 0.5m_0$) and $x_{p,0} = 0.5$ Åfor holes ($\phi_V \approx 4.65$ eV and $m \approx 0.8m_0$). Furthermore, we use the shorthand $E_{AB} = E_A - E_B$ and the auxiliary function

$$\theta(E_{switch}, a, b) = \begin{cases} a & E_{switch} \geqslant 0 \\ b & E_{switch} < 0 \end{cases} \tag{9}$$

to account for the fact that thermal activation is required for hole capture into a trap below E_V while capture in a trap above E_V proceeds without activation (the hole ‘bubbles up’), and vice-versa for electrons.

We take the simplest possible case that can capture the currently available data. We assume that when the defect is in state 1 the trap energy lies at E_T, has a MPE barrier of ΔE_B, and a MPFAT reference field F_c. When in states 2 and 3, the defect level is assumed to be at E_T' with a small charging/discharging MPE barrier ΔE_C. Although the barrier ΔE_C is expected to be considerably lower than the barrier ΔE_B, it is responsible for the E' centers to act as ‘slow states’ in CP measurements. Nonetheless, for the data investigated here, ΔE_C can be neglected. We also neglect the MPFAT mechanism for charging/discharging since our data taken to sense these characteristics are recorded at relatively low fields. Transition from state 3 to state 1 (full annealing rather than electrical neutralization) proceeds over a barrier ΔE_A. Thus, the rates read as follows

$$k_{12} = k_p^c(E_T, \Delta E_B, F_c) + k_n^e(E_T, \Delta E_B, F_c), \tag{10}$$
$$k_{23} = k_p^e(E_T', \Delta E_C, 0) + k_n^c(E_T', \Delta E_C, 0), \tag{11}$$
$$k_{32} = k_p^c(E_T', \Delta E_C, 0) + k_n^e(E_T', \Delta E_C, 0), \tag{12}$$
$$k_{31} = \nu \exp(-\beta\Delta E_A), \tag{13}$$

where the shorthand k(trap level, MPE barrier, MPFAT reference field) is used and $\nu \sim 10^{13}$ Hz is the typical attempt frequency for thermal transitions over energetic barriers.

The transition rates between states 2 and 4 are modeled in the spirit of [1] by thermal activation over a field-dependent barrier (cf. Fig. 4) as

$$k_{24} = \nu e^{-\beta(\Delta E_D - E_2 - \gamma F)}, \tag{14}$$
$$k_{42} = \nu e^{-\beta(\Delta E_D - E_4 + \gamma F)}. \tag{15}$$

Consequently, the probability of being in state 4 corresponds to a positive charge at the E' center *and* a depassivated interface state.

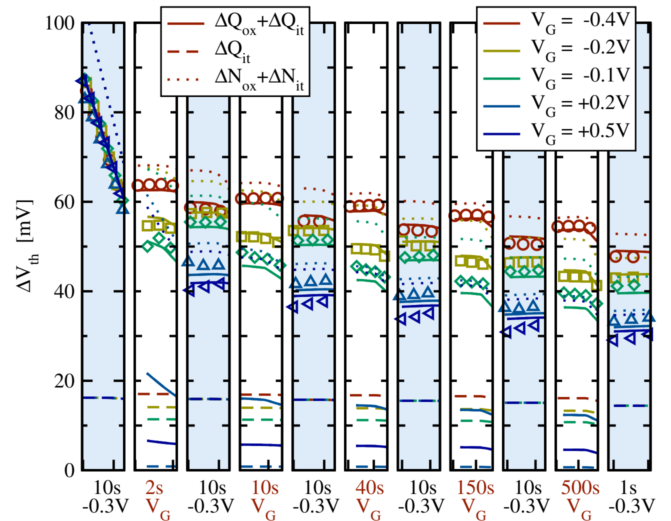

Fig. 7. Five devices were brought to the same level of degradation ($t_s = 6000$ s, $T = 125$ °C, $V_{stress} = -2$ V). First, recovery was monitored for 10 s at $V_G = V_{th} = -0.3$ V (panel 1). Then the gate voltage was switched for 2 s to 5 different values, including more negative and more positive values (panel 2). When possible ($V_G > 0$ V), the change in the drain current was converted to $\Delta V_{th}(V_G)$ which was found to be clearly different from $\Delta V_{th}(V_{th})$ recorded at V_{th}. Next, V_G was switched back to V_{th} (panel 3), were a clear impact of the intermediate bias switch is observed. This procedure was repeated for increasing durations of bias switches (10, 40, 150, 500 s). Simulation results are given by the lines, which show very good agreement with the data, capturing both the occupancy effect (evenly numbered panels) and the acceleration/retardation of recovery as a response to the gate bias.

In order to describe the response of a device to a change in the bias conditions, a certain number of defects N is assumed to exist. Due to the amorphous nature of the Si/SiO_2 interface, each defect will be described by a unique configuration of random energy-levels and the overall created interface and oxide charges are obtained from suitably defined averages.

In order to explain the presently available data, a reduced set of random energy-levels is sufficient and we use $x \approx 0$, $\Delta E_A \approx \Delta E_B$, and $\Delta E_C \approx 0$ in the following examples. Further simplification, like $E_T' \approx E_T$, significantly deteriorates the quality of the model [30].

5. Comparison with measurements

Simulation results for the SiON devices are compared to the data of Fig. 1. The simulated prefactors during stress are in very good agreement with the data, see Fig. 5. Details of the simulation demonstrate also that the model can reproduce the asymmetry between stress and recovery [30]. Details of the simulation demonstrate also that the model can reproduce the asymmetry between stress and recovery, see Fig. 6. We remark that this is the first time that a model can reproduce both OTF and recovery data in a wide temperature and voltage range, providing a theoretical link between these two measurement techniques. Also, good agreement between experiment and model is obtained for high-k and ultra-thick SiO_2 devices [30].

A particularly challenging data set is given in Fig. 7, where five devices are brought to the same level of degradation. During recovery, various bias switches are used to probe both the occupancy effect (amount of charge visible depending on the Fermi-level) as well as the impact of the occupancy on the recovery dynamics. Again, very good agreement between theory and data is obtained.

6. Conclusions

We suggest a two stage model for the negative bias temperature instability based on established properties of E' centers. Creation of

E' centers from their oxygen vacancy precursors is suggested to occur via a *multiphonon-field-assisted* hole trapping mechanism. The created E' centers are then suggested to favor the depassivation of interface states, which results in a coupling of created oxide and interface state component.

This model can explain degradation and recovery over a wide range of bias voltages and stress temperatures, the observed asymmetry between stress and recovery, and the strong sensitivity to bias and temperature during recovery. Excellent agreement with data from three vastly different technologies (thick SiO_2, SiON, and HK) is obtained, supporting the idea that NBTI is determined by the chemistry of the amorphous SiO_2/Si interface region. The model has the minimum number of parameters required to explain the experimentally observed features of NBTI.

Acknowledgements

The research leading to these results has received funding from the European Community's Seventh Framework Programme under Grant agreement No. 216436 (project ATHENIS). We also gratefully acknowledge stimulating discussions with P. Lenahan and A. Shluger.

References

[1] V. Huard, C. Parthasarathy, N. Rallet, C. Guerin, M. Mammase, D. Barge, C. Ouvrard, in: Proceedings of the IEDM, 2007, pp. 797–800.
[2] B. Kaczer, T. Grasser, P. Roussel, J. Martin-Martinez, R. O'Connor, B. O'Sullivan, G. Groeseneken, in: Proceedings of the IRPS, 2008, pp. 20–27.
[3] T. Grasser, in: Proceedings of the IRPS, 2008, (Tutorial).
[4] M. Alam, H. Kufluoglu, D. Varghese, S. Mahapatra, Microelectron. Reliab. 47 (2007) 853.
[5] T. Grasser, B. Kaczer, T. Aichinger, W. Goes, M. Nelhiebel, IIRW Final Report, 2008.
[6] B. Kaczer, V. Arkhipov, R. Degraeve, N. Collaert, G. Groeseneken, M. Goodwin, in: Proceedings of the IRPS, 2005, pp. 381–387.
[7] T. Grasser, B. Kaczer, P. Hehenberger, W. Goes, R. O'Connor, H. Reisinger, W. Gustin, C. Schlünder, in: Proceedings of the IEDM, 2007, pp. 801–804.
[8] T. Grasser, B. Kaczer, W. Goes, in: Proceedings of the IRPS, 2008, pp. 28–38.
[9] T. Tewksbury, Ph.D. Thesis, MIT, 1992.
[10] M. Weissman, Rev. Mod. Phys. 60 (1988) 537.
[11] D. Fleetwood, H. Xiong, Z.-Y. Lu, C. Nicklaw, J. Felix, R. Schrimpf, S. Pantelides, IEEE Trans. Electron. Dev. 49 (2002) 2674.
[12] C. Henry, D. Lang, Phys. Rev. B 15 (1977) 989.
[13] M. Kirton, M. Uren, Adv. Phys. 38 (1989) 367.
[14] S. Makram-Ebeid, M. Lannoo, Phys. Rev. B 25 (1982) 6406.
[15] S. Ganichev, W. Prettl, I. Yassievich, Phys. Solid State 39 (1997) 1703.
[16] E. Poindexter, W. Warren, J. Electrochem. Soc. 142 (1995) 2508.
[17] P. Lenahan, Microelectron. Eng. 69 (2003) 173.
[18] P. Sushko, S. Mukhopadhyay, A. Mysovsky, V. Sulimov, A. Taga, A. Shluger, J. Phys-Condens. Matter 17 (2005) 2115.
[19] A. Lelis, T. Oldham, IEEE Trans. Nucl. Sci. 41 (1994) 1835.
[20] J. Conley Jr., P. Lenahan, A. Lelis, T. Oldham, Appl. Phys. Lett. 67 (1995) 2179.
[21] C. Nicklaw, Z.-Y. Lu, D. Fleetwood, R. Schrimpf, S. Pantelides, IEEE Trans. Nucl. Sci. 49 (2002) 2667.
[22] A.V. Kimmel, P. Sushko, A. Shluger, G. Bersuker, in: R. Sah, J. Zhang, Y. Kamakura, M. Deen, J. Yota, (Eds.), Silicon Nitride, Silicon Dioxide, and Emerging Dielectrics, vol. 10, in press, (ECS Transactions).
[23] S. Mahapatra, K. Ahmed, D. Varghese, A.E. Islam, G. Gupta, L. Madhav, D. Saha, M.A. Alam, in: Proceedings of the IRPS, 2007, pp. 1–9.
[24] V. Reddy, A. Krishnan, A. Marshall, J. Rodriguez, S. Natarajan, T. Rost, S. Krishnan, in: Proceedings of the IRPS, 2002, pp. 248–254.
[25] A. Krishnan, C. Chancellor, S. Chakravarthi, P. Nicollian, V. Reddy, A. Varghese, R. Khamankar, S. Krishnan, in: Proceedings of the IEDM, 2005, pp. 688–691.
[26] D. Ang, S. Wang, G. Du, Y. Hu, IEEE Trans. Dev. Mater. Reliab. 8 (2008) 22.
[27] J. Zhang, Z. Ji, M. Chang, B. Kaczer, G. Groeseneken, in: Proceedings of the IEDM, 2007, pp. 817–820.
[28] G. Kapila, N. Goyal, V. Maheta, C. Olsen, K. Ahmed, S. Mahapatra, in: Proceedings of the IEDM, 2008, pp. 103–106.
[29] B. Kaczer, T. Grasser, J. Martin-Martinez, E. Simoen, M. Aoulaiche, P. Roussel, G. Groeseneken, in: Proceedings of the IRPS, 2009.
[30] T. Grasser, B. Kaczer, W. Goes, T. Aichinger, P. Hehenberger, M. Nelhiebel, in: Proceedings of the IRPS, in press.
[31] J. Campbell, P. Lenahan, C. Cochrane, A. Krishnan, S. Krishnan, IEEE Trans. Dev. Mater. Reliab. 7 (2007) 540.
[32] V. Afanas'ev, A. Stesmans, Eur. Phys. Lett. 53 (2001) 233.
[33] J. Conley Jr., P. Lenahan, W. McArthur, Appl. Phys. Lett. 73 (1998) 2188.
[34] T. Grasser, P.-J. Wagner, P. Hehenberger, W. Goes, B. Kaczer, IEEE Trans. Dev. Mater. Reliab. 8 (2008) 526.